Molecular Crystals and Liquid Crystals

Publication details, including instructions for authors and subscription information:
http://www.tandfonline.com/loi/gmcl20

Liquid Crystal Devices for Photonic Switching Applications: State of the Art and Future Developments

A. D'Alessandro [a] & R. Asquini [a]

[a] Dipartimento di Ingegneria Elettronica, Università degli Studi di Roma, "La Sapienza", Istituto Nazionale di Fisica per la Materia, via, Eudossiana, 18-00184, Roma

Version of record first published: 18 Oct 2010

To cite this article: A. D'Alessandro & R. Asquini (2003): Liquid Crystal Devices for Photonic Switching Applications: State of the Art and Future Developments, Molecular Crystals and Liquid Crystals, 398:1, 207-221

To link to this article: http://dx.doi.org/10.1080/15421400390221682

Mol. Cryst. Liq. Cryst., Vol. 398, pp. 207–221, 2003

ISSN: 1542-1406 print/1563-5287 online
DOI: 10.1080/15421400390221682

Taylor & Francis
Taylor & Francis Group

LIQUID CRYSTAL DEVICES FOR PHOTONIC SWITCHING APPLICATIONS: STATE OF THE ART AND FUTURE DEVELOPMENTS

A. d'Alessandro and R. Asquini
Dipartimento di Ingegneria Elettronica, Università degli Studi di Roma, "La Sapienza", Istituto Nazionale di Fisica per la Materia, via, Eudossiana, 18-00184 Roma

Liquid crystal devices to perform optical switching, filtering and to build optical crossconnects for wavelength division multiplexed optical communication systems are reviewed. Basic working principle of both devices already commercialised and those ones still at laboratory stage reported in the recent scientific literature are described. Devices based on liquid crystals and those ones made by using alternative technologies (MEMS, lithium niobate, semiconductors) are compared in terms of advantages and disadvantages. Technology issues to fabricate liquid crystal based photonic devices are discussed. Recent results of both free-space and waveguided based liquid crystal optical devices along with novel device concepts using optical channel waveguides are reported.

Keywords: optical switches; surface stabilised ferroelectric liquid crystals

INTRODUCTION

New communication services (TV on demand, video conferencing, high definition cable TV) and ever increasing use of internet require high bandwidth which can be available only by using optical fiber networks.

The degree of connectivity has been increasing lately therefore optical transport networks require large switching systems to route and process photonic signals without cumbersome and costly electro-optic conversion. In particular switching matrices are required to make optical crossconnect systems at nodes of network operating at several wavelengths in the C-band (1530–1560 nm) of minimum losses of optical fibers as in recent wavelength division multiplexed networks.

Specifications for optical switches include large number of input and output ports (up to 1024×1024), switching time below 10 ms, low driving power, polarization independence operation, high level of optical and electronic integration. None of the available technologies can satisfy all of

such requirements. Optical switches based on electrooptic effect in inorganic materials, such as $LiNbO_3$ in waveguide geometries do not allow for fabrication of many inputs and many outputs switching matrices, because of lack of reliability and reproducibility over large areas and for high losses [1]. Micro-electro-mechanical switches based on vertical torsion of micromirrors on Si substrate seem to be a promising solution to implement large switching matrices operating with free-space propagating collimated beams, but high driving voltages in the order of several tens of volts are required to get switching times below 10 ms [2] and matrix dimension is limited by diffraction losses of expanding Gaussian beams in free-space. Analog or 3D MEMS offer higher number of ports but alignment is critical and complicated drivers are needed. Another proposed technology consists of so called "bubble-switch" in which total internal reflection is obtained by switching the refractive index of a substance, when it goes from vapour to liquid phase, placed at cross-points of silica waveguides. The maximum dimension of bubble switch matrices are limited by high losses and high driving currents necessary to maintain the state of a bubble [3]. A further approach for switching technology is based on thermo-optic effect which can be used in passive materials such as glass and was largely exploited to make space-division optical switches with Mach-Zehnder interferometer configuration, based on planar lightwave circuit technology. It employs silica-based waveguides on silicon, but high driving power of the order of 0.4 W is required [4].

Liquid crystals (LC) are interesting materials to make optical switches both in free-space and waveguided structures [5]. Main advantages in using LC's are their transparency in the near infrared spectrum for any data formats, they have high birefringence, refractive index ranging between 1.4 and 1.6 as in silica optical fibers and low loss optical waveguides (such as in glass, silica on silicon, polymers). Furthermore LC's are cost effective since small quantities of materials are necessary to process a large number of devices over large areas as demonstrated by the mature flat panel display technology. Ferroelectric liquid crystals (FLC) add other advantages such as bistability in surface stabilised cells, high speed response times ranging between 10 and 100 μs, high-efficiency electro-optic effect, low absorption and scattering losses in the range of 2 dB/cm [6]. Optical switches using LC can be classified into two main classes: I) SLM based free-space switches and II) integrated optic waveguided switches. The switches belonging to the former class are based either on polarization conversion of light through a twisted nematic (TN) LC cell or on beam steering by digital holograms electrically written in FLC-SLM.

In this paper the state of the art of optical switching made by using LC's is reviewed. Optical switching systems based on spatial light modulators (SLM) and waveguided switches are illustrated and compared.

LIQUID CRYSTAL FREE-SPACE SWITCHES

Figure 1 shows a polarization independent optical switch made of two single pixel TN LC cells and two polarization beam splitters/combiners used to allow polarization diversity scheme, as adopted by Spectraswitch commercial devices [7]. The polarization beam splitters work in such a way that horizontal polarization passes through undeflected and vertical polarization passes through with a deflection. In such a device an incoming arbitrarily polarized light beam is decomposed into two orthogonal polarizations, vertical and horizontal, by the first polarization beam splitter. When a voltage is applied to the TN LC cell, as in Figure 1a, no polarization conversion of light occurs and the two light beams are recombined by the second polarization beam splitter acting as a combiner into a light signal routed to output A.

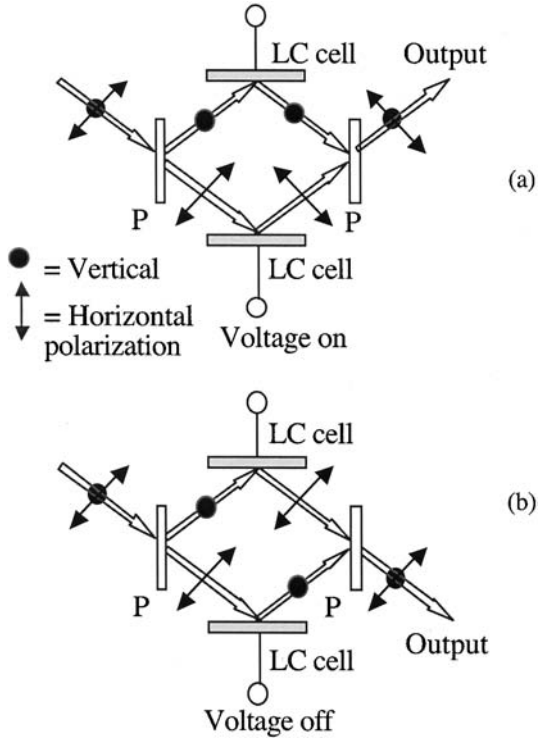

FIGURE 1 Sketch of a polarization independent switch made by using TN LC cells as polarization converters: (a) voltage is applied to the LC cell and no polarization conversion occurs; (b) voltage is not applied and polarization conversion of light occurs.

In the case no voltage is applied to the TN LC cell, as in Figure 1b, polarization conversion of light occurs and the two light beams are recombined by the second polarization beam splitter/combiner into a light signal routed to output B. Based on this scheme, one input–two outputs and two inputs–two outputs devices, named WaveWalker™, have been made and commercialized by Spectraswitch.

Table 1 shows some features of WaveWalker™ performance. It is worth to notice low crosstalk and insertion loss. The same working principle can be extended by using multiple pixel cells to make LC switches for wavelength division multiplexed (WDM) systems. As in the device proposed by Patel and Sibelberg a WDM light beam is dispersed by a grating, acting as a demultiplexer, into single light beams, each of a single wavelength, each collimated onto a single pixel of TN LC display cell. Each pixel behaves as a polarization converter and can process each wavelength separately and different wavelengths can be routed to different output ports [8], according to the same scheme reported in Figure 1 for polarization independence. Corning has engineered this device which is characterized by excellent channel isolation but paid in terms of expensive bulk optics components required to assemble the overall switch.

An alternative approach to make optical switch matrices with a large number of input and output ports uses holographic optical beam deflectors based on binary and multiple-phase LC-SLM [9].

Figure 2 shows the block scheme of the "ROSES" project demonstrator, a 1×8 switch, which uses a hologram recorded onto a ferroelectric liquid crystal over silicon spatial light modulator (FLC/Si SLM), to steer the incoming beam to the desired output port. The FLC/Si SLM is configured as a reflective half-wave plate and the FLC allows to record binary-phase holograms. The device also includes a waveguide array (WGA) which provides the input and output ports, a custom-made opto-mechanical

TABLE 1 Specifications of Spectraswitch WaveWalker™

Insertion loss	<1.0 dB
Nominal crosstalk	−40 dB
Polarization dependent loss	0.1 dB
Return loss	45 dB
Operating temperature	−5° to 70°C
Nominal switching time	4 ms
Maximum switching rate	100 Hz
Maximum input optical power	300 mW
Wavelength range	C band
Power supply	±12 Vdc
Control	TTL

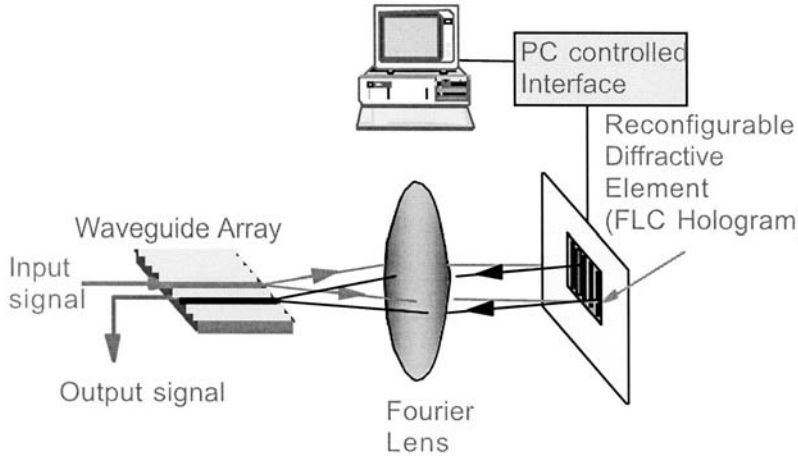

FIGURE 2 Block scheme of the "ROSES" project demonstrator based on a FLC/Si SLM [9] (© 2000 IEEE and courtesy of Cambridge University Engineering Department Photonic Group).

mount with six-axis alignment adjusters which houses the WGA and a single collimation/transform lens. A computer is interfaced to drive the FLC/Si SLM and to interconnect the input to the desired output. The device is reconfigurable and the approach allows for easy port scaling.

The picture of Figure 3a shows an overall view of the device including SLM, fibers, optics and drivers. Figure 3b shows in particular the binary array and the SRAM drive circuitry made on Si backplane.

The SLM consists of a linear array of 540 pixellated ITO electrodes, each $18\,\mu m \times 6\,mm$, with $2\,\mu m$ dead space between the pixels. Light incident on the SLM passes through the FLC layer, is reflected from the aluminium mirror and then passes back through the liquid crystal layer. The first-order diffraction efficiency of a binaryphase hologram with FLC layer thickness d, and molecular tilt angle θ is given by:

$$\eta = \sin^2 2\theta \cdot \sin^2\left(\frac{2\pi\Delta n d}{\lambda}\right) \tag{1}$$

where Δn is the birefringence and λ is the operating wavelength.

Equation (1) shows that efficiency is maximized when the device acts as a half-wave plate in reflection at the wavelength of operation (1550 nm), and the ferroelectric tilt angle is 45°. One problem is that an high tilt angle in a FLC material is not compatible with the presence of SmA phase [10]. The absence of the SmA phase has two consequences. Firstly two equivalent orientations of FLC molecules appear and alignment technique,

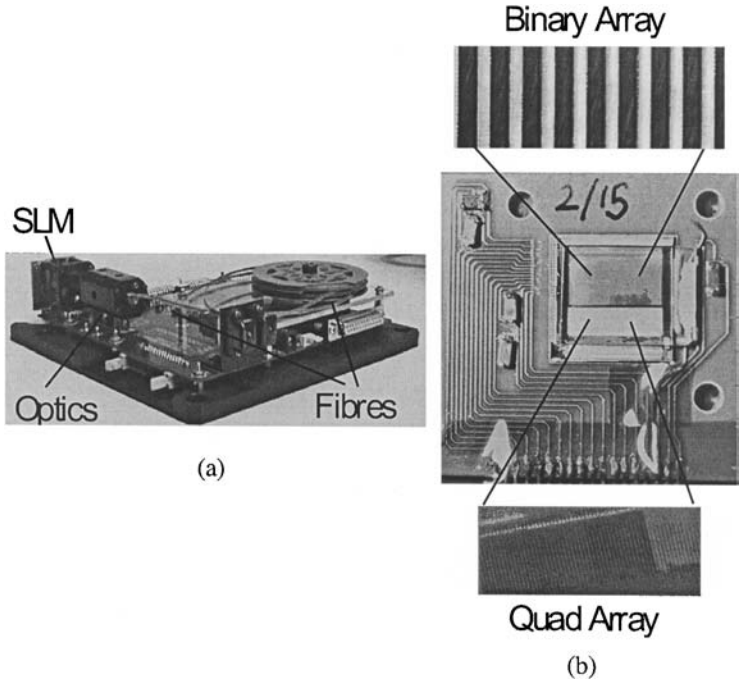

FIGURE 3 "ROSES" demonstrator: (a) overview of the switch including fibers, drivers and optics; (b) picture of the SLM/Si [9]. (© 2000 IEEE and courtesy of Cambridge University Engineering Department Photonic Group).

using rubbed polyimmides as Nylon 6–6, must provide the selection of one of the orientations. Secondly the FLC is not bistable but monostable with consequent disadvantage for the addressing schemes to be used. On the other hand a high tilt angle FLC, in comparison with standard FLC materials, have a tilt angle which is almost temperature independent and consequently the switch performance are not affected by temperature variations.

Thickness of the FLC layer is 3.5 μm, at least three times thicker than FLC layers for display applications operating at visible wavelengths, since birefringence at infrared wavelengths is lower than in the visible spectrum. Higher thicknesses imply decrease of the switching speed of the material. FLC mixtures used for the ROSES demonstrator are CS2005 by Chisso with 45° tilt angle and CDRR8, an organosiloxane-based experimental compound synthesised by Goodby at Hull University, U.K., with tilt angle of 34° at room temperature. Performance figures for 1×8 switch are 16.9 dB insertion loss and −19.1 dB isolation. Losses are mainly due to ITO

absorption and can be reduced by using thinner layers of ITO and fine tuning design of the optics. Typical drive field of 8–10 V/μm at 500 Hz is provided by SRAM integrated circuits and a 50 μs reconfiguration speed was achieved.

FLC/SLM's have been also used in a Banyan network architecture to make a reconfigurable wavelength add-drop filter [11]. The Banyan network is an interconnection network that has important applications for partitioning of multiprocessor systems, digital optical computing, and optical fiber communication systems. It was first proposed as an efficient interconnection network for multiprocessor partitioning applications. Specifically, these switching stages use total internal reflection (TIR) prisms with ferroelectric liquid crystal (FLC) polarization rotators to form compact modules. Using this Banyan network implementation, a reconfigurable multiwavelength add-drop filter for wavelength division multiplexed (WDM) applications was proposed [11].

Experimental results show that the 2×2 FLC-based polarization-dependent switch has 6.7 dB average insertion loss, 35.3 μs switching time, and about 40 dB average ON–OFF interchannel crosstalk. It is expected that the insertion loss will be less than 2 dB by optimized design engineering.

WAVEGUIDED LIQUID CRYSTAL SWITCHES

Several integrated optics devices using nematic and ferroelectric liquid crystals with optical waveguides were proposed and experimentally demonstrated. Some of waveguided liquid crystal devices using LC perform amplitude modulation of light at low frequencies, in the range of few kHz. These devices use a simple structure consisting of an FLC layer path between input and output slab waveguides as reported in [12] and [13]. Recently Hermann *et al.* demonstrated that promising integrated optic devices with FLC can be fabricated by using low loss polymeric waveguides [14]. The main advantage in using polymeric waveguides consists of depositing a polymeric buffer layer between ITO and the optical waveguide in order to reduce losses due to ITO absorption especially at wavelengths of C-band of interest for optical communications [15]. Modulation of light amplitude was also demonstrated by employing an active FLC cladding overlaying an optical waveguide as proposed in [16] and [17]. An integrated optical switch was demonstrated in which a light beam in a polymer waveguide can be switched towards either of two distinct output ports by means of total internal reflection by changing refractive index of a nematic LC used as overlayer [18]. Optical waveguides made of SSFLCs were also used to perform beam-steering, by exploiting double-refraction effect and $1 \times N$ optical switches can be thus envisaged by employing a proper

electrode design [19]. Clark and Handschy first demonstrated an integrated optical switch based on a surface stabilized ferroelectric liquid crystal (SSFLC) layer sandwiched between two ion-exchanged glass multimode optical waveguides to form a sort of vertical directional coupler [20]. In such a device, FLC molecules are reoriented by applying an electric field which induces a change of refractive index n_{FLC} of the FLC coupling layer. Light travels undisturbed in the input waveguide (bar state of the switch) when $n_{FLC} < n_W$, n_W being the waveguide refractive index. Light can be transferred to the other arm of the directional coupler (cross-state of the switch) when $n_{FLC} > n_W$. A vertical directional coupler based switch using an FLC as intermediate layer between two optical waveguides was also simulated by using beam propagation method (BPM) and ultra-short coupling lengths in the order of 100 μm were figured out [21]. Such a coupling length is much shorter than that one obtained in regular directional couplers (in which refractive index of the layer between waveguides is equal to the refractive index of the substrate) made by using other technological approaches (e.g. lithium niobate, semiconductors, etc.). Vertical directional couplers using nematic LC were also demonstrated both theoretically [22-23] and experimentally [24]. In the sample reported in ref. [20] the FLC layer was aligned by shearing technique and ITO electrodes were deposited on external surfaces of only 150 μm thick glass substrates used as buffer. Such thin substrates were used to reduce high driving voltage due to external electrodes. Nevertheless light could be switched from one waveguide to another by applying no less than 1 kV [20]. In another technological solution single mode, rather than multimode, waveguides and a thin layer of 200 Å of ITO for electrodes were used to make the vertical directional coupler [25] consisting of an SSFLC cell made of two BK7 glass substrates. Two single mode optical waveguides have been obtained on the inner surfaces of the cell by using ion-exchange process. Indium tin oxide electrodes with a thickness of 200 Å and 4 mm^2 have been deposited by electron-beam vacuum evaporation and covered by a 400 Å layer of teflon, as alignment layer, deposited by hot friction. The cell was assembled with 1.8 μm gap filled with ferroelectric liquid crystal M4851-025 by Hoechst.

Beam propagation calculations were carried out to find out the values of n_w and n_{FLC} to get maximum optical power transferred from one waveguide to another in the cross-state [26]. In particular an optimum effective refractive index $n_w = 1.528$ at the wavelength of 0.6328 μm was obtained by performing ion-exchange at 385°C for 10 min in a salt mixture made of an initial mixture of $NaNO_3$:KNO_3 50% by weight and adding 0.7 mole% of $AgNO_3$. The corresponding optimum value of $n_{FLC} = 1.533$ in the cross-state was obtained by choosing an orientation of teflon with an angle of 19° respect to the propagation direction. This optimized alignment orientation was computed for FLC extraordinary refractive index 1.611, ordinary

refractive index 1.466 and tilt angle of 26° at temperature of 25°C. A picture of the realized prototype on optical bench is reported in Figure 4, where input and output SF6 coupling prisms are also included.

Among lightwave FLC switches a unique feature of such a device is the bistability of its optical response which reduces even further its driving power in system applications.

A value of maximum on–off extinction ratio ER_{max} over 15 dB and a residual one ER_{res} about 9 dB after FLC relaxation were measured for driving peak voltage of about 23 V applied to the prototype reported in Figure 4. A value of ER_{max} over 14 dB was measured even for peak voltage of just 5 V [25]. Furthermore such values of extinction ratios can be greatly improved by obtaining a better alignment uniformity. In fact an optical inspection of the SSFLC cell revealed small domains which were not able to switch because of poor alignment. The device insertion losses were measured and resulted 5.5 dB, including about 0.8 dB due to Fresnel losses of the coupling prisms and also including the glass waveguide propagation losses of about 2 dB/cm. Switching of light between the two waveguides can be performed in about 270 μs switching time [27].

The complete switching area is less than 4 mm long which is nevertheless shorter than coupling length of commercial electro-optic coupler-based switches made of $LiNbO_3$ [1]. Coupling length of the SSFLC optical switch can be further reduced by using a photolithographic mask to pattern

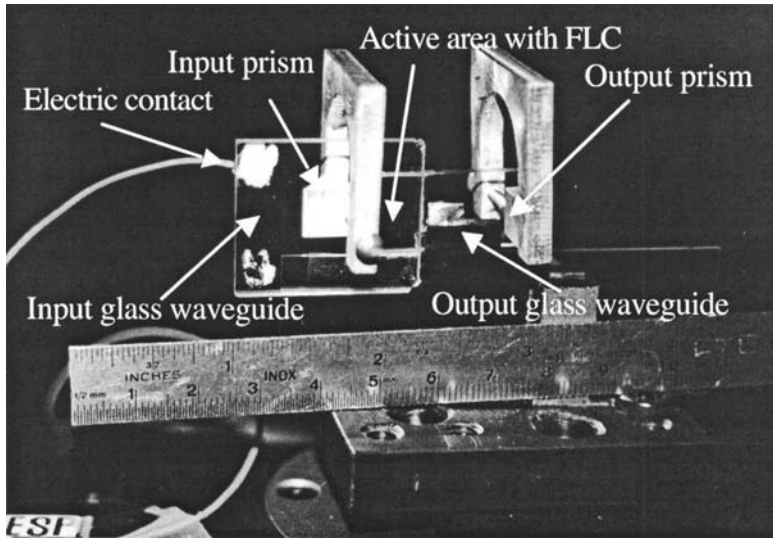

FIGURE 4 Picture of a SSFLC vertical directional coupler switch prototype with coupling prisms.

the electrodes with better resolution. Simulations of the device by BPM indicates that coupling length as short as 60 μm can be achieved [24].

This device concept can be easily extended by using display technology to make large optical switch matrices for cross-connects in optical networks. In particular channel waveguides can be used to arrange a large number of switches to obtain multiport switch matrices. Hermann demonstrated the advantage in using polymeric materials both for buffer and waveguide layers to make SSFLC integrated optic devices [14]. In particular photoresist-like polymers can be used to pattern low loss optical channel waveguides, whose refractive index can be tailored by slightly changing the polymer composition.

Recently low loss channel waveguides with losses as low as 0.5 dB/cm measured at 1550 nm were fabricated by using different compositions of P(PFS-GMA) (poly(pentafluorostyrenecoglycidylmethacrylate)) [28]. These polymers have been used to design a vertical directional coupler SSFLC optical switch operating in the C-band. In particular the multilayer structure of the coupler includes a 6 μm thick polymeric buffer placed between waveguides and ITO electrodes (20 nm thick), a 5 μm thick FLC layer and an alignment layer of 40 nm [29]. The design was carried out by using BPM and optimization was obtained by studying the extinction ratio ER, defined as the ratio of the optical power at waveguide outputs in the cross-state and losses referred to the ratio between the output and input power.

The BPM simulations showed that an optimized device can be obtained with an extinction ratio ER of more than 50 dB and losses less then 1 dB with coupling length of only 174 μm, using 3 μm thick polymeric waveguides, with a refractive index of 1.475 at 1550 nm.

The losses are very low due to the buffer effect which avoids absorption of ITO. These calculations served as starting point to design a novel integrated optic device configuration using channel waveguides with bending paths in order to allow fiber optic coupling and to build large optical switch matrices. In fact starting from the 2D results, a 3D structure has been considered to study the width of the channel waveguides and the width of the ITO electrodes.

The modal properties of waveguides at 1550 nm have been studied and a width of 6 μm has been chosen in order to get single mode propagation. Then the computed mode which presents an effective index $n_{eff} = 1.46648$ has been launched into the optimised 3D structure. Different devices with ITO electrode width (W_{ITO}) varying from 6 μm to 16 μm have been simulated in order to obtain high extinction ratios (ER) at the output waveguides and low losses.

The results of simulations are summerized in Table 2, divided into two parts related to ER, losses and coupling length (L_c): the first part (ER_{Max}, Losses and L_c) with shaded background refers to optimized device design

TABLE 2 Performance of Integrated Optic Waveguide Switches with SSFLC and Polymeric Waveguides

W_{ITO} [μm]	ER_{Max} [dB]	Losses [dB]	L_c [μm]	ER [dB]	$Losses_{min}$ [dB]	L_c [μm]
6	32.11	1.96	269.8	16.91	0.42	216
7	63.55	1.96	255.4	17.42	0.35	205.8
8	33.44	1.96	246.6	17.77	0.32	198.8
9	26.73	1.92	240.2	18.09	0.31	194.8
10	22.74	1.76	233.8	18.6	0.33	192.2
11	23.27	2.7	140.8	19.24	0.41	190.8
12	24.81	2.85	133.4	19.96	0.53	189
13	26.11	2.95	138.8	20.66	0.66	187.6
14	27.13	3.01	138.6	21.22	0.79	186.4
15	27.99	3.05	138.4	21.48	0.88	185.6
16	28.67	3.06	138.4	21.5	0.93	185

with the maximum extinction ratio, the second part (ER, $Losses_{min}$, L_c) with white background refers to the same devices with shorter lengths and minimum losses. The first part of Table 2 shows that a maximum $ER_{Max} = 63.55$ dB can be obtained for $W_{ITO} = 7$ μm, with losses of 1.96 dB at a coupling length $L_c = 255.4$ μm . The same device, cut at a shorter length, shows lower losses paid in terms of a reduced ER. Minimum losses of 0.35 dB at $L_c = 205.8$ μm can be obtained but with ER = 17.42 dB as reported in second part of Table 2.

The calculated ER along the propagation direction z along with the optical losses for the device with $W_{ITO} = 7$ μm are plotted in Figure 5. Table 2 and Figure 5 show that good compromises between ER and losses can be achieved.

Using the results obtained studying the single 3D optical switch and the results of theoretical calculations [4] of the bending losses applied to our waveguides, an optical path of a 2×2 optical switch with a 13 μm ITO width and $L_c = 187.6$ μm have been simulated.

Figure 6 shows the pathway and the cross section in the active area of the entire switch. The dashed lines refer to the waveguides in the lower substrate and the solid lines refer to the waveguides in the upper one. The bent waveguides are arcs of 45° with 6 mm radius, and each arc of waveguide shows radiation losses of about 0.02 dB. The bends have been designed as a sequence of arcs connected by lateral offsets to minimize transition losses. The optical power evolution at 1550 nm along the pathway from input waveguide 1 to output waveguide 2′ is reported in Figure 7.

We obtained losses as low as 0.75 dB for the complete path with an efficient transfer of light from input 1 to output 2′. The device can be

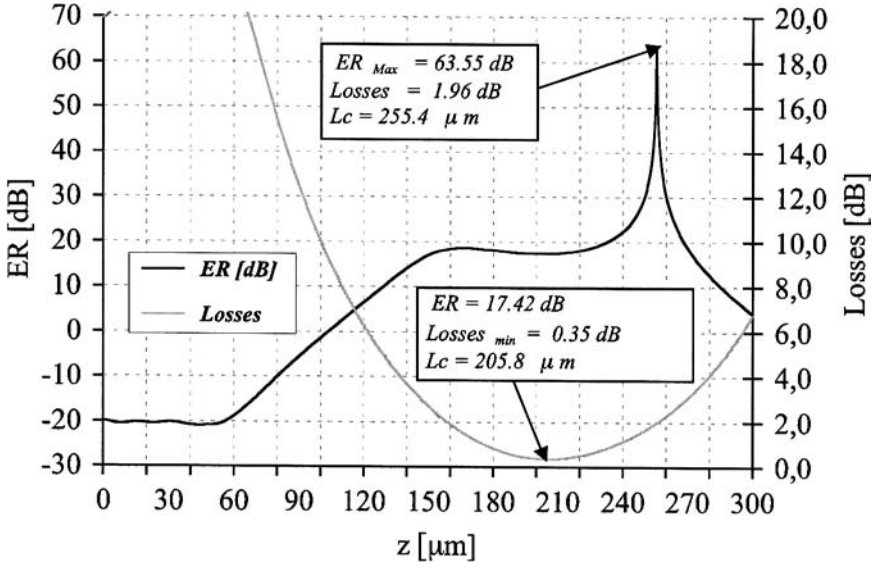

FIGURE 5 Evolution of extinction ratio (ER) and losses along propagation direction z of an integrated optic switch, whose simulation data are reported in the text.

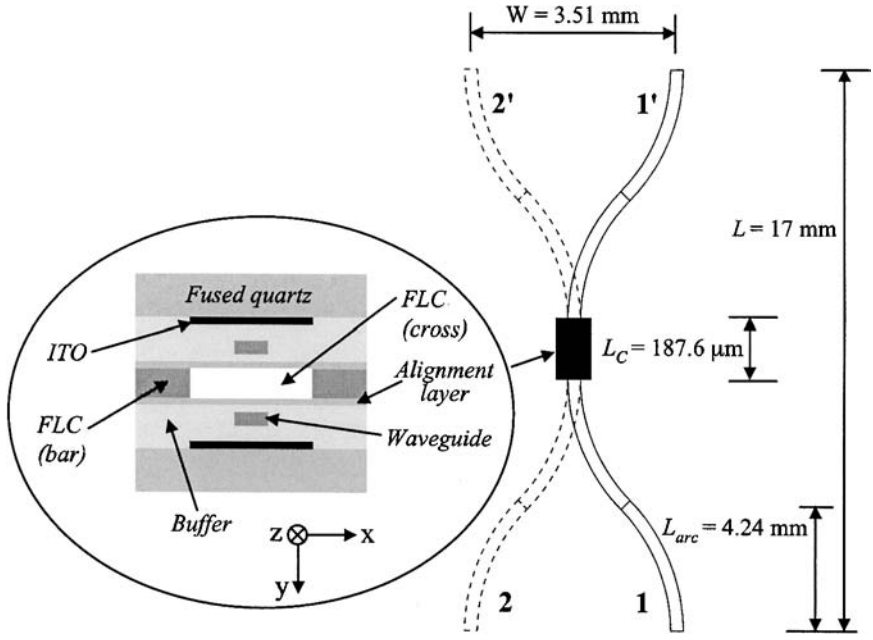

FIGURE 6 Sketch of an integrated optic switch with SSLFC and two bent polymeric waveguides placed in the upper (solid) and lower substrates (dashed). The inset shows the cross section of the multilayer structure of the switch.

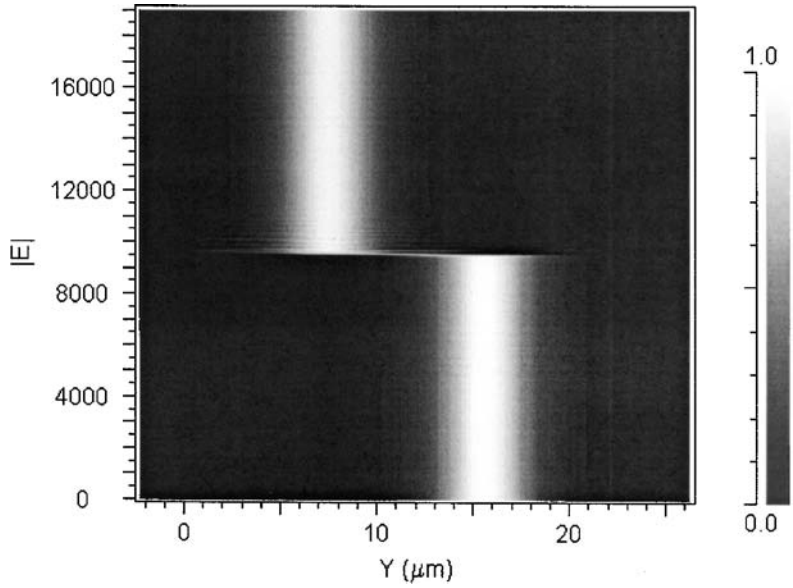

FIGURE 7 Evolution of optical power along the propagation direction of the structure of Figure 6 from input 1 to output 2′.

further improved by optimizing the thicknesses of the different layers. A prototype of such a device is under construction.

CONCLUSIONS

Liquid crystals have interesting properties to make optical switches using both free-space and waveguided approaches with promising performance. Liquid crystal switches in general are easily scalable by using large area technology for flat panel displays. Moreover novel LC devices for optical switching recently demonstrated include electrically switchable gratings by using either PDLC [30] or dye-doped LC's [31] or LC-polymers composite materials [32]. Integrated optical devices can be obtained by using LC and various waveguide technologies: polymeric, glass and silica on silicon waveguides. Further research and engineering efforts are required to bring laboratory prototypes to commercial stage by reducing insertion losses above all and optimizing optical properties of LC materials for wavelengths of interest for optical communications.

REFERENCES

[1] Murphy, E. J., Murphy, T. O., Ambrose, A. F., Irvin, R. W., Lee, B. H., Peng, P., Richards, G. W., & Yorinks, A. (1996). *J. Lightwave Technol.*, *14* (3), 352–358.

[2] Lee, S., Huang, L., Kim, C., & Wu, M. C. (1999) *J. Lightwave Technol.*, (1999). *17* (1), 7–13.

[3] Fouquet, J. E. (2000). *Optical Fiber Communication Conf. 2000*, *1*, 204–206.

[4] Goh, T., Yasu, M., Hattori, K., Himeno, A., Okuno, M., & Ohmori, Y. (2001). *J. Lightwave Technol.*, *19* (3), 371–379.

[5] Hirabayashi, K. & Kurokawa, T. (1993). *Liq. Cryst.*, *14* (2), 307–317.

[6] Giallorenzi, T. G., Weiss, J. A., & Sheridan, J. P. (1976). *J. Appl. Phys.*, *47* (5), 1820–1826.

[7] http://www.spectraswitch.com.

[8] Patel, J. S. & Sibelberg, Y. (1995). *IEEE Photon. Technol. Lett.*, *7* (5), 514–516.

[9] Crossland, W. A., Manolis, I. G., Redmond, M. M., Tan, K. L., Wilkinson, T. D., Holmes, M. J., Parker, T. R., Chu, H. H., Croucher, J., Handerek, V. A., Warr, S. T., Robertson, B., Bonas, I. G., Franklin, R., Stace, C., White, H. J., Woolley R. A., & Henshall, G. (2000). *J. Lightwave Technol.*, *18* (12), 1845–1853.

[10] Collings, P. J. & Hird, M. (1997). *Introduction to Liquid Crystal Chemistry and Physics*, Taylor and Francis: New York.

[11] Riza, N. A. & Shifu Yuan. (1999). *J. Lightwave Technol.*, *17* (9), 1575–1584.

[12] Walker, D. B., Glytsis, E. N., & Gaylord, T. K. (1996). *Applied Optics*, *35* (16), 3016–3030.

[13] Scalia, G., Hermann, D. S., Abbate, G., Komitov, L., Mormile, P., Righini, G. C., & Sirleto, L. (1998). *Mol. Cryst. Liq. Cryst.*, *320*, 321–335.

[14] Hermann, D. S., Scalia, G., Pitois, C., De Marco, F., D'havé, K., Abbate, G., Lindgren, M., & Hult, A. (2001). *Opt. Engin.*, *40* (10), 2188–2198.

[15] Hamberg, I. & Granqvist, C. G. (1986). *J. Appl. Phys.*, *60* (11), 123–159.

[16] Ozaki, M., Sadohara, Y., Hatai, T., & Yoshino, K. (1990). *Jap. J. Appl. Phys.*, *29* (5), 843–845.

[17] Ozaki, M., Sadohara, Y., Uchiyama, Y., Utsumi, M., & Yoshino, K. (1997). *Liquid Crystals*, *14* (2), 381–387.

[18] Kobayashi, M., Terui, H., Kawachi, M., & Noda, J. (1982). *IEEE J. Quantum Electron.*, *18* (10), 1603–1610.

[19] Gros, E. & Dupont, L. (2001). *IEEE Photon. Technol. Lett.*, *13* (2), 115–117.

[20] Clark, N. A. & Handschy, M. A. (1990). *Appl. Phys. Lett.*, *57* (18), 1852–1854.

[21] Lee, W. Y., Lin, J. S., Lee, K. Y., & Cheung, W. C. (1995). *J. Lightwave Technol.*, *13* (11), 2236–2243.

[22] Lee, W. Y., Lin, J. S., & Cheung, W. C. (1995). *J. Lightwave Technol.*, *14*, 2547–2553.

[23] Lin, K., Chuang, W., & Lee, W. (1996). *J. Lightwave Technol.*, *14*, 2547–2553.

[24] Muto, S., Nagata, T., Asai, K., Ashizawa, H., & Arh, K. (1990). *Jpn. J. Appl. Phys.*, *29*, 1724–1726.

[25] d'Alessandro, A., Asquini, R., Menichella, M., & Ciminelli, C. (2001). *Mol. Cryst. Liq. Cryst.*, *372*, 353–363.

[26] d'Alessandro, A., D'Orazio, A., Campoli, F., Petruzzelli, V., Chessa, G., & Maltese, P. (1998). *Mol. Cryst. Liq. Cryst.*, *320*, 355–364.

[27] Asquini, R. & d'Alessandro, A. (2000). *Proc. LEOS 2000*, paper MM4, *1*, 119–120.

[28] Pitois, C., Vukmirovic, S., Hult, A., Wiesmann, D., & Robertsson, M. (1999). *Macromol.*, *32*, 2903–2909.

[29] Asquini, R. & d'Alessandro, A. (2002). *Mol. Cryst. Liq. Cryst.*, *372*, 243–251.

[30] Simoni, F. & Francescangeli, O. (2000). *Int. J. of Polym. Mat.*, *45*, 381–449.
[31] Kaczmarek, M., Shih, M. Y., Cudney, R. S., & Khoo, I. C. (2002). *IEEE J. Quant. Electron.*, *38*, 451–457.
[32] Caputo, R., Sukhov, A. V., Tabiryan, V., Umeton, C. P., & Ushakov, R. F. (2001). *Chemical Physics*, *271*, 323–335.